Analyst

PAPER

View Article Online
View Journal | View Issue

Cite this: *Analyst*, 2025, **150**, 4572

Determination of airborne metal-containing nanoparticles in a historic mining area using single particle ICP-MS†

Tjaša Žerdoner,[a,b] Janja Vidmar, *[a,b] Bor Arah[c] and Tea Zuliani *[a,b]

Given limited information on airborne metal-containing NPs—a highly bioaccessible fraction of metals relevant to human exposure—in the upper Meža Valley, a historic mining area in Slovenia, this study aimed to assess their presence in PM_{10} air filters from the region using the spICP-MS method. The extraction procedure, refined using a certified reference material of PM_{10}-like fine dust deposited on filters, achieved an extraction efficiency of 9.1% for Zn- and 14.0% for Pb-containing NPs after two hours of ultrasonication in 10 mM sodium pyrophosphate. The method proved effective for detecting metal-containing NPs in PM_{10} from mining and smelting areas, as demonstrated by a case study from the upper Meža Valley. SpICP-MS analyses identified both Zn- and Pb-containing NPs in PM_{10} samples, with 0.6–3.8% of Zn and 0.3–1.7% of Pb extracted as NPs. Additionally, SEM-EDS analysis confirmed the presence of Zn- and Pb-containing (nano)particles of different chemical compositions. This study is the first to report the occurrence of metal-containing NPs in PM_{10} from this region. Although they represent only a small fraction of total Zn and Pb in the samples, NPs are more bioaccessible and thus more relevant for assessing local population's exposure to these particles.

Received 29th April 2025,
Accepted 20th May 2025

DOI: 10.1039/d5an00480b

rsc.li/analyst

1. Introduction

The presence of persistent contaminants in the environment, primarily generated by human activities such as agriculture, traffic, industry, and mining, poses a significant global threat to ecosystems and human health. These contaminants can be transported through the air, facilitated by suspended particles like aerosols and dust to which substances with low volatility may be attached. This airborne transport serves as an important pathway for the redistribution of contaminants from localized sources to larger environmental areas. One of the main contributors to air pollution is airborne particulate matter (PM), which is a complex mixture of solids and aerosols composed of particles that vary in size, shape, and chemical composition. Based on their size, PM can be classified into three categories, including PM_{10} (coarse particles with diameters smaller than 10 μm), $PM_{2.5}$ (fine particles with diameters smaller than 2.5 μm), and $PM_{0.1}$, which is also referred to as ultrafine particles or atmospheric nanoparticles, describing particles with diameters smaller than 100 nm. The hazard posed by PM to humans is highly dependent on its size and size distribution. PM_{10} has been linked to adverse health effects such as respiratory and cardiovascular diseases.[1] A study by Liu *et al.*, covering over 600 cities in multiple countries, found that a 10 μg m^{-3} increase in the 2-day average of PM_{10} concentration was associated with a 0.44% rise in daily all-cause mortality, a 0.36% increase in daily cardiovascular mortality, and a 0.47% increase in daily respiratory mortality.[2] $PM_{0.1}$, which are also known as airborne nanoparticles (NPs), present an even greater concern, as they can remain suspended in the air for longer periods and be transported over longer distances. Due to their small size, they can be inhaled into much deeper regions of the lungs and can enter the bloodstream very quickly and efficiently. NPs are also more susceptible to biological uptake and, therefore, most relevant in terms of bioavailability.[3] Moreover, PM may mobilize very high concentrations of potentially toxic elements (PTEs) such as Pb, As, Zn, and Cd, which can, after deposition, accumulate in soil, water, and vegetation. Some PTEs are carcinogenic (*e.g.,* As, Cd, Cr) and can impact nervous function, damage vital organs, and cause DNA damage. Long-term exposure to these elements is linked to Alzheimer's and Parkinson's diseases, muscular dystrophy, and multiple sclerosis.[4] For instance, exposure to Pb can cause neurotoxic effects

[a]*Jožef Stefan International Postgraduate School, Jamova 39, Ljubljana, Slovenia*
[b]*Jožef Stefan Institute, Department of Environmental Sciences, Jamova 39, Ljubljana, Slovenia. E-mail: janja.vidmar@ijs.si, tea.zuliani@ijs.si*
[c]*Jožef Stefan Institute, Center for Electron Microscopy and Microanalysis, Jamova 39, Ljubljana, Slovenia*

† Electronic supplementary information (ESI) available. See DOI: https://doi.org/10.1039/d5an00480b

such as learning or behavioral problems, including speech, intelligence, attention, behavior, and mental processing problems, particularly in children.[5]

As metal-containing NPs form a growing category of substances found in the atmosphere with implications for human health, understanding their occurrence, fate, and behavior in the environment is essential. For this purpose, suitable analytical techniques for collecting airborne NPs and determining their concentration, chemical composition, and size are of paramount importance. Airborne NPs are typically collected using air sampling filters made of *e.g.*, quartz, teflon, or polycarbonate, or by using cascade impactors, electrostatic or thermal precipitators, and liquid impingers, to name a few, each tailored to capture particles of different sizes and specific analysis needs. Filters designed for PM sampling effectively collect a wide range of particle sizes, including NPs ($PM_{0.1}$). The collected samples can be analyzed using gravimetric analysis to determine the total mass of PM, electron microscopy to assess the particle size and morphology, and energy-dispersive X-ray spectroscopy or inductively coupled plasma mass spectrometry (ICP-MS) to determine their chemical composition. Most of these techniques lack the sensitivity or selectivity required to detect target NPs, which are often present at low concentrations, among a mixture of particles with varying sizes and chemical compositions naturally found in the PM matrix. ICP-MS only offers data on the elemental composition of bulk PM samples, rather than on individual NPs. However, when operated in single particle (sp) mode, spICP-MS extends its capability by providing information on the size and concentration of individual NPs within the PM. SpICP-MS has been recognized as a suitable method for studying the occurrence of metal-containing NPs at environmentally relevant concentrations, offering sensitive and element-specific detection of NPs.[6–8] This is achieved by utilizing the established elemental analysis capabilities of ICP-MS while performing measurements on an individual particle basis.[9,10] In principle, a liquid sample containing NPs must be diluted sufficiently to ensure that the NPs enter the plasma individually, where they are vaporized, atomized, and ionized. The resulting positively charged ion packets are then transported to the detector, which records them as signal bursts by monitoring fast transient signals, with each burst corresponding to a single NP. The size of each burst is proportional to the mass of NPs, while the frequency of these bursts corresponds to the particle number concentration. By combining this data with information on the particle composition, shape, and density, the size and size distribution of NPs can be obtained. The spICP-MS method therefore provides simultaneous quantification of NP mass concentration, size characterization of NPs, and allows the detection of both dissolved and particulate forms of an element. Due to the ability to differentiate between dissolved and nanoparticulate forms, spICP-MS allows monitoring of the potential dissolution of NPs during the sample treatment. It also provides valuable data on the particle number concentration, which is a very relevant measure of exposure to airborne NPs.

To measure airborne metal-containing NPs using spICP-MS, both online and offline approaches for sampling and detection have been applied. Cen *et al.* demonstrated the applicability of a rotating disk diluter coupled with spICP-MS for direct sampling, online dilution, and characterization of airborne NPs.[11] However, since the proposed setup is not widely accessible in most analytical laboratories, offline methods are more commonly used. This involves collecting airborne NPs on PM filters, from which they are subsequently extracted into a liquid phase for analysis by spICP-MS. It is important that the extraction process efficiently recovers NPs from PM samples and at the same time does not create conditions whereby particle aggregation/agglomeration or dissolution occurs, leading to the loss of NPs. Therefore, strong acids that could dissolve the NPs should be avoided. Current methods for extracting NPs from PM filters typically involve aqueous extraction by immersing filters in water or other extraction solutions, often combined with ultrasonication to aid in dislodging the NPs from the filter surface. For instance, Bland *et al.* employed ultrasound-assisted extraction in deionized water to analyze $PM_{2.5}$ filters for metal-containing particles.[12] Similarly, Torregrosa *et al.* explored different extraction approaches (*e.g.,* direct immersion, hard cap espresso, ultrasound-assisted, and microwave-assisted extraction) and different extraction solvents (including trisodium citrate, ammonium hydroxide, potassium nitrate, *etc.*) to recover artificially deposited standards of AuNPs and PtNPs from air filters.[13]

The limited number of existing studies on the spICP-MS analysis of metal-containing NPs in PM air filters and similar environmental samples, such as road dust, either do not report on the efficiency of the extraction procedure, or the extraction recoveries reported are not quantitative.[6,12,14] The estimation of trueness is a key aspect of validating any analytical procedure that consists of an extraction method and subsequent analysis. However, few if any studies have evaluated the trueness of spICP-MS for determining airborne NPs, which is partially due to the lack of certified reference materials (CRMs) with known NPs concentration and size in a PM matrix. In the absence of such CRMs, an alternative approach for assessing trueness could involve spiking a PM matrix with a known amount of (certified reference) standards of target NPs with defined particle sizes, as has been done for other environmental matrices such as road dust, road runoff sediments, and soils.[14–16] However, there are currently very few CRMs available for pristine metal-containing NPs, whether in suspension or powder form, that can be used for spiking. Moreover, the detailed validation of the method may not be needed if the scientific objective of the study is simply to establish the presence or absence of NPs in a certain environmental matrix.

The upper Meža Valley in Slovenia is heavily polluted with potentially toxic elements (PTEs) due to its history of mining and smelting lead and zinc ore, along with the large volumes of mining waste that have been deposited in the area.[17–20] In addition to the high concentrations of PTEs found in the soil

and sediments, the inhabitants of the area are exposed to these elements daily, mainly by inhalation and/or ingestion of dust. Regular monitoring of Pb concentrations in PM_{10} by the Slovenian Environment Agency in Žerjav, where a Pb smelter used to operate and where a Pb-recycling and Pb-battery production site is now located, showed an increase in Pb annual average concentrations from 250 to 700 ng m^{-3} between 2010 and 2021.[21] Although the region has been extensively studied for the presence of PTEs, there have been no reports on their occurrence in the form of NPs in PM, which, if inhaled, could be highly bioaccessible and pose a potential risk to human health.[22]

Therefore, the aim of this study was to assess the presence of metal-containing NPs in PM_{10} air filters collected from the upper Meža Valley using the spICP-MS method. The focus was on Zn-, Pb-, As-, and Cd-containing NPs, as they are the most likely to occur in the PM_{10} from mining and smelting areas. To achieve that, the method of extraction of NPs from PM_{10} collected on filters was improved. For this purpose, a certified reference material of PM_{10}-like fine dust, closely reflecting the composition of real PM_{10} samples, was deposited onto PM_{10} quartz fiber filters, and the ultrasound-assisted extraction of metal-containing NPs was refined for their subsequent analysis by spICP-MS. The results of this study, therefore, offer additional insights into the presence, concentration, and size characteristics of airborne metal-containing NPs in areas heavily affected by mining activities.

2. Materials and methods

2.1. Collection of PM_{10} samples

PM_{10} samples were collected in the upper Meža Valley, in the town of Žerjav, at two different sampling locations and in two different years (2018 and 2021), as detailed in Table S1.† Sampling at location 1 (in 2018) was performed using a high-volume DIGITEL DHA-80 sampler with 150 mm quartz fiber filters. The filters were changed automatically every 24 hours at a predetermined time. The airflow through the filter was 720 m^3 day^{-1}. Sampling at location 2 (in 2021) was performed using a reference low-volume sampler, Leckel SEQ 47/50, with pre-annealed 47 mm quartz fiber filters. The filters were changed automatically every 24 hours at a predetermined time. The airflow through the filter was 55.2 m^3 day^{-1}. The filter size and airflow did not impact the amount of PM collected, as the surface area-to-airflow ratio was comparable between the locations. The amount of PM collected on the filters for all samples ranged from 1 to 2 mg, depending on the levels of PM_{10} in the environment on a given day. For filters of smaller sizes (47 mm from location 2), the entire filter was used for extraction and subsequent spICP-MS analysis, allowing for only one replicate. The filters of larger sizes (150 mm from location 1) were cut into two circles before analysis, each with a diameter comparable to the smaller filters, enabling two replicates for analysis. All filters were dried overnight at 60 °C and weighed before the analysis.

2.2. Extraction of NPs from PM_{10} samples

The procedure used for extracting metal-containing NPs from PM_{10} filters was based on ultrasound sonication, which has been previously reported as an effective approach for the extraction of PM from air filters.[12,13,23] The two parameters further optimized in this study were the sonication time and the type of extraction solvent (MilliQ water, 10 mM sodium pyrophosphate, 1% citric acid, and 1% aqueous ammonia solution), while the concentrations of extraction solvents were adapted from the work of Torregrosa *et al.*[13] The sonication times of 0.5 h, 1 h, and 2 h were tested with 10 mM sodium pyrophosphate, which proved to be the most suitable extraction solvent (please refer to the Section 3.1.2). The extraction procedure was optimized using the PM_{10} quartz fiber filters (MN QF-10, 47 mm, Macherey-Nagel, Düren, Germany), onto which a suspension of certified reference material ERM-CZ120 (PM_{10}-like fine dust, obtained from European Commission Joint Research Centre, Geel, Belgium) was applied. ERM-CZ120 is certified for a total concentration of Zn (1240 mg kg^{-1}), Pb (113 ± 17 mg kg^{-1}), As (7.1 ± 0.7 mg kg^{-1}), and Cd (0.90 ± 0.22 mg kg^{-1}). The ERM-CZ120 suspension was prepared by weighing 20 mg of ERM-CZ120 powder into 50 mL of MilliQ water, resulting in a 0.4 mg mL^{-1} PM_{10}-like fine dust suspension. The resulting suspension was sonicated using an ultrasonic bath, operated at 40 kHz for 30 min. Five mL of the ERM-CZ120 suspension were applied to PM_{10} filters, retaining approximately 2 mg of PM_{10}-like fine dust. A schematic of the extraction optimization procedure is shown in Fig. S1.†

The optimized extraction procedure involved placing dried quartz filters containing approximately 2 mg of PM_{10} collected in the upper Meža valley into 50 mL polypropylene (PP) graduated tubes to which 20mL of 10 mM sodium pyrophosphate was added. The samples were subjected to bath sonication (Sonis, Iskra PIO, Šentjernej, Slovenia), operated at 40 kHz frequency for 2 h. The extracts were afterward quantitatively transferred to 30 mL PP graduated tubes, while the filters and 50 mL tubes were rinsed with 5 mL of sodium pyrophosphate, which was combined with the rest of the extract. During the extraction, the filters partially disintegrated, resulting in the presence of filter fibers in the extracts. As this could lead to clogging of the ICP-MS nebulizer, the fibers needed to be removed before spICP-MS analysis. Since the centrifugation could not remove quartz fibers from the extracts, filtration through 12–25 μm black ribbon filters (Schleicher&Schuell GmbH, Dassel, Germany) was applied. To minimize the risk of adsorptive losses of metal-containing NPs, the 12–25 μm filters were first pre-equilibrated. This involved passing 5 mL of MilliQ water and 1 mL of the sodium pyrophosphate through the filter and discarding the solution. This step was repeated three times to ensure proper filter pre-equilibration before filtering the extracts.

2.3. Determination of total element concentration in PM_{10} samples and extracts

To follow the mass balance of the extraction procedure, the total concentration of Zn, Pb, Cd, and As in each extraction

step was determined using ICP-MS following microwave-assisted digestion, as described in the ESI.† The samples analyzed included quartz filters with PM_{10} samples before and after extraction (dried overnight at 60 °C), solutions of the extracts, filtered extracts (passed through 12–25 μm filters), and the ERM-CZ120 water suspension. After digestion, samples were diluted with MilliQ water (resulting in a 1% HNO_3 solution) and subsequently analyzed using a 7700× quadrupole ICP-MS instrument (Agilent Technologies, Tokyo, Japan). ICP-MS operating parameters, presented in Table S2,† were optimized daily for the highest sensitivity. Quantification was based on external calibration by measuring Zn, Pb, Cd, and As ionic standards prepared in 1% HNO_3, covering the concentration range of 0.5–500 μg L^{-1}, and an online internal standard of 25 μg L^{-1} Rh in 1% HNO_3. A multielement standard solution Multi VI, containing 1000 mg L^{-1} of Zn, Pb, Cd, and As, and single element standard solutions of 1000 mg L^{-1} Rh from Merck Ltd were used for calibration. Each sample was digested in parallel. A certified reference material for trace elements in surface water (SPS-SW1, Spectrapure standards, Oslo, Norway) was used to verify the accuracy of the ICP-MS analysis. The measured values were in good agreement with the certified values (Table S3†). The filtrates (*i.e.*, solutions passing through the quartz filter during the deposition of the ERM-CZ120 suspension onto the filters) were acidified with 20 μL of concentrated HNO_3 and measured directly by ICP-MS to determine whether any element was retained on the quartz filter.

2.4. Single particle ICP-MS analysis of extracted NPs

SpICP-MS analyses of metal-containing NPs, including those containing Zn, Pb, As, and Cd, were performed in the filtered extracts on a 7900x quadrupole ICP-MS instrument (Agilent Technologies). SpICP-MS operating parameters, presented in Table S2,† were optimized daily for the highest sensitivity. A multi-element batch was used for consecutive measurements of four elements in time-resolved mode. The signal intensity of the ^{66}Zn, ^{208}Pb, ^{75}As, and ^{111}Cd isotopes was recorded consecutively for 60 s for each isotope with a dwell time of 0.1 ms. An accurate sample flow rate was determined daily by weighing MilliQ water introduced as a sample at a peristaltic pump speed of 0.1 rotations per second ($N = 3$). Before spICP-MS analysis, the sample extracts were diluted with MilliQ water (2× for extracts in MilliQ water and 1% citric acid, 5× for extracts in 1% aqueous ammonia solution, and 10× for extracts in 10 mM sodium pyrophosphate) to ensure that the number of particles detected during one acquisition time ranged between 100 and 2000. This adjustment aimed to detect a sufficient number of particles for statistical purposes, while minimizing bias due to multiple particle events. Another consideration in selecting the optimal dilution factor was to maintain a low baseline signal, which could otherwise be increased due to spectral interferences and/or the presence of dissolved analytes (as in the case of the extraction with 1% citric acid).

As the concentrations of As- and Cd-containing NPs in the filter extracts were below the detection limit, only Zn- and Pb-containing NPs were quantitatively analyzed by spICP-MS. The transport efficiency was determined daily according to the particle size method.[24] This involved analyzing a 50 nm AuNP suspension prepared from a stock suspension (BBI Solutions, Cardiff, UK), which contained 56.8 mg L^{-1} of citric-acid-coated AuNPs with an average particle diameter of 50 ± 3 nm, diluted to a concentration of 0.142 μg L^{-1}. Additionally, ionic Au standards (prepared from a single Au ICP Standard Certipur form Merck Ltd) were prepared at concentrations of 0 μg L^{-1}, 0.5 μg L^{-1}, 1.0 μg L^{-1}, and 5.0 μg L^{-1}. Particle mass quantification was based on calibration curves prepared from different concentration levels of ionic Zn and Pb standards (ranging from 0.5 μg L^{-1} to 100 μg L^{-1}). The impact of four extraction solvents on the transport efficiency, ICP-MS response, and linearity of ionic standard calibration curves was thoroughly investigated, as detailed in the ESI (Table S4†). Briefly, the particle size method was selected for calculating transport efficiency by analyzing AuNP and ionic Au standards prepared in MilliQ water. The particle size method was selected as the particle diameter of the AuNPs in the stock standard solution used to determine transport efficiency is less susceptible to change over time compared to the particle number concentration. The latter can decrease over the storage time of the AuNPs stock solution due to aggregation/agglomeration, particle settling, and/or particle adhesion to the container walls. The ICP-MS ionic response for NPs in MilliQ water, sodium pyrophosphate, and citric acid was determined using matrix-matched ionic standards, whereas the ionic standards for NPs in aqueous ammonia solution were prepared in 0.1% aqueous HNO_3. Particle mass was converted to particle diameter by assuming spherical mono-elemental particles consisting of Zn (Zn mass fraction 1.0, with a density of 7.13 g cm^{-3}) or Pb (Pb mass fraction 1.0, with a density of 11.35 g cm^{-3}). These assumptions introduce significant bias in determining particle sizes, potentially leading to their underestimation. As a result, the particle size information reported by spICP-MS in this study is only qualitative. For creating particle size distribution graphs, bin sizes of 5 nm and 2 nm were used for Zn- and Pb-containing NPs, respectively.

Data processing was performed using the Single Nanoparticle Application Module within the MassHunter 5.2 Workstation Software (Version D.01.02, Build 708.1, Agilent Technologies) in the "Peak Integration Mode". The smallest particle diameter observed in the particle size distribution of filter extracts was considered as the minimum detectable particle diameter. The lowest signal intensity threshold above which events were considered to be NPs was manually set at a value corresponding to a particle diameter of 55 nm for Zn- and 18 nm for Pb-containing NPs (*i.e.*, smallest particle size LODs observed in filter extracts using MilliQ water – please see Table S7†). The application of the same threshold for all samples ensured that a direct comparison of particle mass and number concentrations, as well as median particle diameters, was possible between samples. The mass fraction of Zn- and Pb-containing NPs in PM_{10} samples was calculated by comparing the particle mass concentration determined by

spICP-MS with the total Zn and Pb mass concentration determined in digested samples by ICP-MS. Moreover, Pearson correlation coefficients (PCC) were calculated to assess potential correlations between the particle number or mass concentration and the total mass concentration of the corresponding elements determined in the PM_{10} samples from the upper Meža Valley. The summary of all calculations used in this study is presented in the ESI (eqn (S1)–(S10)†).

2.5. SEM-EDS analysis of the extracted NPs

As the spICP-MS technique requires information on the NP composition, shape, and density for accurate sizing, the shape, size, and elemental composition of Zn- and Pb-containing NPs in the filtered extracts were determined by scanning electron microscopy-energy dispersive spectroscopy (SEM-EDS) in the backscattered electron (BSE) and secondary electron (SE) modes. For this purpose, Verios G4 HP SEM (Thermo Fisher Scientific, Waltham, MA, USA) coupled with an AZtec Live EDS system (Oxford Instruments, Abingdon, UK) was used. EDS measurements were performed with a resolution of around 1 μm, which did not allow the chemical composition of individual particles to be investigated at lower dimensions. Further details on sample preparation and EDS measurements are provided in the ESI.†

3. Results and discussion

3.1. Extraction procedure optimization

The first objective of this study was to further improve the extraction of metal-containing NPs from PM_{10} samples based on the ultrasound-assisted procedure adapted from the existing literature[12,13,23] for their subsequent analysis by spICP-MS. To the best of our knowledge, no certified reference materials for metal-containing NPs in a PM matrix or pristine (certified reference) standards for the target NPs exist for spiking the corresponding PM matrix. Therefore, in this study, the optimization of the extraction procedure was performed using a certified reference material of PM_{10}-like fine dust (ERM-CZ120), which closely mimics the composition of real PM_{10} samples and has a consistent and homogenous composition of Zn, Pb, As, and Cd. However, this material is only certified for the total concentration of the target elements and lacks information on the potential presence or absence of these elements in nanoparticulate form. According to the certification report, the particle size distribution of ERM-CZ120 material, as determined by dynamic light scattering (DLS) in a dispersion, indicates the aerodynamic diameter of the particles, consisting of 10 vol% of particles below 1.75 μm, 16 vol% below 2.49 μm, 50 vol% below 7.59 μm, 84 vol% below 15.01 μm, and 90 vol% below 20 μm.[25] However, the chemical composition of these particles and the percentage of particles smaller than 100 nm is unknown. The presence of NPs containing Zn, Pb, As, and Cd was therefore assessed by spICP-MS analysis of the ERM-CZ120 material suspended in MilliQ water. For this assessment, dilution factors of 500× were applied for Zn- and Pb-containing NPs, and 5× for Cd- and As-containing NPs. Since the concentrations of As- and Cd-containing NPs were below the detection limit (only 1 Cd-containing particle and 4 As-containing particles were detected in the 5× diluted sample), only Zn- and Pb-containing NPs were analyzed quantitatively. The particle number and mass concentrations, particle diameter, and mass fraction of Zn- and Pb-containing NPs determined by spICP-MS in the ERM-CZ120 water suspension are given in Table S5.† The mass concentration of Zn and Pb present in the ERM-CZ120 as NPs was found to be 65.3 mg of Zn-containing NPs per kg of the sample (representing 5.26% of the total Zn content in ERM-CZ120) and 12.8 mg of Pb-containing NPs per kg of the sample (corresponding to 11.3% of the total Pb content in ERM-CZ120). The mean particle sizes, calculated from particle mass based on the assumption of spherical mono-elemental particles, were determined to be 87 nm for Zn- and 32 nm for Pb-containing NPs. The particle number-based size distribution obtained by spICP-MS analysis of the ERM-CZ120 water suspension (Fig. S4†) shows that the sizes of Zn-containing NPs range from 55 nm to over 200 nm, while those of Pb-containing NPs range from 18 nm to more than 100 nm. However, different geometry and chemical composition would result in different particle diameters.

3.1.1. Optimization of extraction duration. The ERM-CZ120 material characterized for the presence of Zn- and Pb-containing NPs (described above) was applied to quartz fiber filters, and NPs were extracted into solution using the ultrasound-assisted extraction procedure, as described in Section 2.2. Different extraction durations (30 min, 1 h, 2 h) were tested using 10 mM sodium pyrophosphate as the extraction solvent to achieve the highest extraction efficiency (Fig. S5†). While longer sonication times correlated with increased extraction of Pb-containing NPs, no clear trend was observed for Zn-containing NPs, leading to the conservative selection of a 2 hour sonication time for further testing.

3.1.2. Optimization of extraction solvent. To further improve extraction efficiency, several solvents were tested, including MilliQ water, 10 mM sodium pyrophosphate, 1% citric acid, and 1% aqueous ammonia solution. After the extraction in different solvents, total Zn and Pb concentrations were first determined by ICP-MS in different fractions, including the filtrate (*i.e.*, the solution that passed through the filter during the application of the ERM-CZ120 suspension), the extracts, and the filters after extraction, to follow the mass balance of the extraction procedure. The results presented in Fig. 1 showed that most of the Zn and Pb were retained on the filters during the deposition of the ERM-CZ120 suspension, with only about 2% passing through. This demonstrated that the quartz fiber filter with deposited ERM-CZ120 was a suitable test material for optimizing the procedure for extracting airborne particles, offering a reliable approximation of the PM_{10} samples. The highest percentage of total Zn in the extract was achieved in 10 mM sodium pyrophosphate (90%), while 1% citric acid was most effective for Pb (66%), followed by 10 mM sodium pyrophosphate (55%). However, the standard deviation of the calculated fractions was high (up to

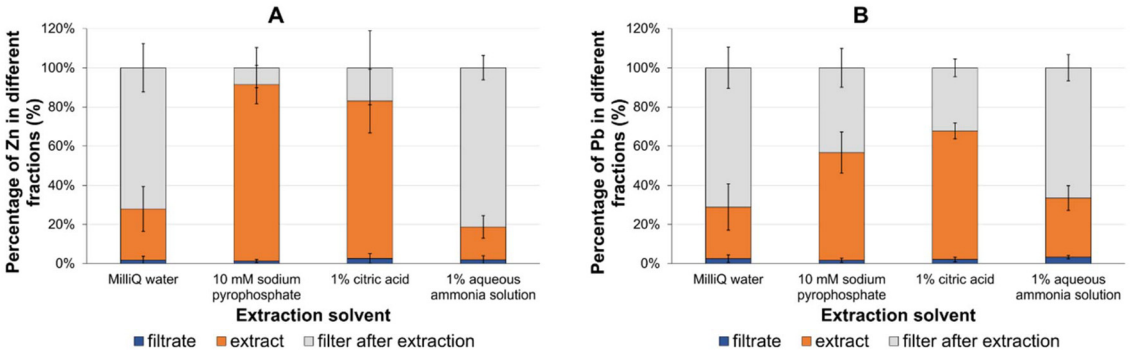

Fig. 1 Percentage of total (A) Zn and (B) Pb concentration determined in different fractions after extraction of ERM-CZ120 from PM_{10} filters using different extraction solvents. The average value and standard deviation were calculated from 6 replicates for each extraction solvent. Zn and Pb concentrations determined in different fractions were normalized to the sum of Zn and Pb concentrations determined by ICP-MS in all fractions.

20%), especially in the case of Zn, as some of the replicate measurements were below the detection limit.

To achieve higher accuracy and precision in quantifying Zn- and Pb-containing NPs in air samples at environmentally low concentrations, a spICP-MS method was applied, offering more sensitive detection of NPs compared to the ICP-MS determination of total element content (Tables S6 and S7†). Before spICP-MS analysis, the extracts were filtered through a 12–25 μm filter to remove the fibers of the partially disintegrated quartz filters. The unwanted retention of NPs on the 12–25 μm filter was checked by comparing the number of particles in the filtered ERM-CZ120 water suspension with those in the unfiltered suspension. The results showed that 68 ± 9% of the Zn- and Pb-containing particles passed through the filter, with good filtration repeatability and without altering the particle size distribution (Fig. S6†). After filtration, the particle concentrations and size distributions of Zn- and Pb-containing NPs extracted from PM_{10} samples were determined by spICP-MS. Table 1 shows the extraction recoveries of Zn- and Pb-containing NPs extracted from PM_{10} filters with ERM-CZ120 using the four extraction solvents. The extraction recovery was calculated by comparing the concentration of Zn- and Pb-containing NPs in the extracts, as determined by spICP-MS, with their expected concentration in the ERM-CZ120 sample deposited on the quartz filter, following the equations eqn (S9) and (S10).† The highest extraction recoveries based on particle mass concentrations for Zn- and Pb-containing NPs were achieved in 10 mM sodium pyrophosphate (9.14% and 14.0%, respectively), followed by 1% aqueous ammonia solution (6.61% and 7.21%, respectively), while the lowest extraction recoveries were obtained in 1% citric acid (2.95% for Zn- and 2.92% for Pb-containing NPs). A similar trend was observed for particle number concentrations, with sodium pyrophosphate showing the highest efficiency (11.0% for Zn- and 21.8% for Pb-containing NPs). These results differ from the findings of Torregrosa *et al.*, who reported better recoveries for extracting PtNPs from micro quartz filters using direct immersion in a 1% aqueous ammonia solution (20.1 ± 1.3%) and a 9 ± 2% recovery in 1% disodium pyrophosphate.[13] Similar to our findings, the lowest recovery was reported for 1% citric acid (1.12 ± 0.18%). In the same study, the authors reported 84 ± 2% recoveries achieved

Table 1 Extraction recovery based on particle number and mass concentration, mean particle size, and mass fraction of Zn- and Pb-containing NPs in ERM-CZ120 extracted from PM_{10} filters using different extraction solvents. Results represent the average values with a standard deviation of six replicates

	Zn				Pb			
	Extraction recovery[a] (%)				Extraction recovery[a] (%)			
Extraction solvent	Based on particle number conc.	Based on particle mass conc.	Mean particle size (nm)	Mass fraction of NPs[b] (%)	Based on particle number conc.	Based on particle mass conc.	Mean particle size (nm)	Mass fraction of NPs[b] (%)
MilliQ water	5.25 ± 3.14	3.57 ± 1.36	82 ± 4	3.80 ± 0.30	6.84 ± 3.14	4.24 ± 2.01	30 ± 1	6.99 ± 4.19
10 mM sodium pyrophosphate	11.0 ± 2.9	9.14 ± 2.69	94 ± 2	1.96 ± 0.67	21.8 ± 3.0	14.0 ± 3.4	28 ± 1	7.12 ± 0.88
1% citric acid	0.737 ± 0.189	2.95 ± 1.29	152 ± 10	0.157 ± 0.075	0.857 ± 0.166	2.92 ± 1.18	54 ± 4	0.185 ± 0.062
1% aqueous ammonia solution	11.2 ± 4.2	6.61 ± 2.45	85 ± 1	5.46 ± 1.64	8.85 ± 2.95	7.21 ± 1.98	29 ± 1	29.6 ± 10.9

[a] Extraction recovery was calculated following eqn (S9) and (S10).† [b] Mass fraction of NPs was calculated following eqn (S8).†

after ultrasound-assisted extraction of PtNPs from filters in ammonia solution. This is significantly higher compared to the extraction recoveries obtained in our study after applying ultrasound-assisted extraction of ERM-CZ120 from filters in 10 mM sodium pyrophosphate. It is important to note that the recoveries reported by Torregrosa *et al.* were obtained for suspensions of manufactured single-element NPs applied to air filters. In contrast, our study used certified reference material resembling PM_{10}-like fine dust, which more accurately reflects the composition of real PM_{10} samples. Specifically, matrix effects from airborne PM retained on the filter can influence the accuracy and precision of NPs determination, as also demonstrated by Torregrosa *et al.*[13] Therefore, it is more appropriate to compare our method's performance with studies that have extracted and detected metal-containing NPs from more realistic environmental samples. For example, Folens *et al.* quantified PtNPs in road dust by spICP-MS following an ultrasonication extraction procedure using stormwater runoff for leaching.[6] The authors reported an extraction efficiency of 2.7%, which is as low as those obtained in our study. Similarly, Avramescu *et al.* reported an extraction efficiency of 1.28 ± 0.14% for a road dust composite spiked with CeO_2 NPs following water extraction with sonication.[14] The authors selected water as an extractant to isolate only the readily bioavailable NPs from the road dust. In our study, higher extraction recoveries for Zn- and Pb-containing NPs in PM_{10} samples were achieved using sodium pyrophosphate, which enhances NPs extraction and promotes their dispersion. In summary, the recoveries observed in our study cannot be considered low, especially when compared to the studies referenced above, which report similar or lower extraction efficiencies for various types of NPs from different environmental samples.

The influence of different extraction solvents on the size and size distribution of the extracted NPs was further investigated. The mean particle sizes (Table 1) and particle size distributions (Fig. 2) of Zn- and Pb-containing NPs in ERM-CZ120 extracted from PM_{10} filters with MilliQ water, 10 mM sodium pyrophosphate, and 1% aqueous ammonia solution were similar to those in ERM-CZ120 suspended in the corresponding extraction solvents (Table S5†). This suggests that extraction in these solvents had little impact on particle size, meaning it did not cause significant aggregation, dissolution, or selective size fractionation. In contrast, extraction with 1% citric acid resulted in significantly larger mean particle sizes (152 nm for Zn- and 54 nm for Pb-containing NPs) compared to other extraction solvents and the ERM-CZ120 suspended in 0.5% citric acid (90 nm for Zn- and 34 nm for Pb-containing NPs, Table S5†). The size distribution for particles extracted with 1% citric acid also shifted towards larger sizes (Fig. 2C and G), most likely due to partial dissolution of Zn- and Pb-containing NPs, as evidenced by the increased baseline signal for Zn and Pb after extraction (Fig. S7†). Consequently, a higher particle detection threshold had to be applied, resulting in elevated size LOD (114 nm for Zn- and 41 nm for Pb-containing NPs after extraction with 1% citric acid, *versus* approximately 65 nm for Zn- and 20 nm for Pb-containing NPs after extraction with other solvents) (Table S7†).

As can be further evidenced from Table 1, the mass fraction of Zn- and Pb-containing NPs was the highest in 1% aqueous ammonia solution, followed by MilliQ water and 10 mM sodium pyrophosphate, and the lowest in 1% citric acid. The mass fractions of Zn- and Pb-containing NPs in ERM-CZ120 after extraction from the filters (*e.g.*, 3.80% for Zn- and 6.99% for Pb-containing NPs in MilliQ water) were generally lower than those obtained for the suspensions in the corresponding extraction solvents (*e.g.*, 5.26% for Zn- and 11.3% for Pb-containing NPs in MilliQ water) (Table S5†). This could indicate selective particle size fractionation during the application of the ERM-CZ120 suspension to the quartz filters, approximately 30% particle loss due to filtration of the extract through a 12–25 μm filter, and/or particle dissolution during extraction, particularly with 1% citric acid.

Summing up, the highest percentages of extracted Zn and Pb in both total and nanoparticulate fractions were achieved using 10 mM sodium pyrophosphate without affecting the particle size distribution. The optimized extraction procedure involved sonication of the PM_{10} filter in 10 mM sodium pyrophosphate for 2 h, followed by filtration of the extract through a pre-conditioned 12–25 μm filter.

3.2. Determination of total element concentration in PM_{10} samples from the upper Meža Valley

The total mass concentration of elements in seven PM_{10} samples, collected at different locations and times (Table S1†), was determined by summing the element concentrations measured in the extracts and filters after extraction (see eqn (S1)–(S4)†). Only Zn and Pb were detected in the samples, while the concentrations of As and Cd were below the detection limit. The total Zn and Pb concentrations in the collected PM_{10} samples ranged from 857 to 1848 mg kg^{-1} and from 3798 to 26 413 mg kg^{-1}, respectively, as shown in Table 2. While the Zn concentrations in the collected samples were similar to those in the ERM-CZ120 material (1240 mg kg^{-1}), the Pb content was significantly higher compared to the ERM-CZ120 (113 ± 17 mg kg^{-1}), indicating the possible contribution of Pb to air pollution in the upper Meža Valley. The total concentrations of both Zn and Pb were significantly higher on the PM_{10} samples collected in June and August 2021 at location 2 (samples 4, 5, 6, and 7) compared to the samples collected in October 2018 at location 1 (samples 1, 2, and 3). The observed differences in Zn and Pb concentrations may be attributed to the location and/or the presence of Saharan dust, which was elevated in June 2021. In June 2021, the Slovenian Environment Agency reported increased PM_{10} levels, along with elevated concentrations of some elements, particularly Al and Fe, due to the presence of Saharan dust across Slovenia.[26] The latter could lead to an increased amount of PM_{10} to which elements can be attached.[27,28]

To compare the obtained results with the annual limit value of Pb in airborne PM,[29,30] set to 500 ng m^{-3}, the total Zn and Pb mass concentrations per volume of filtered air were cal-

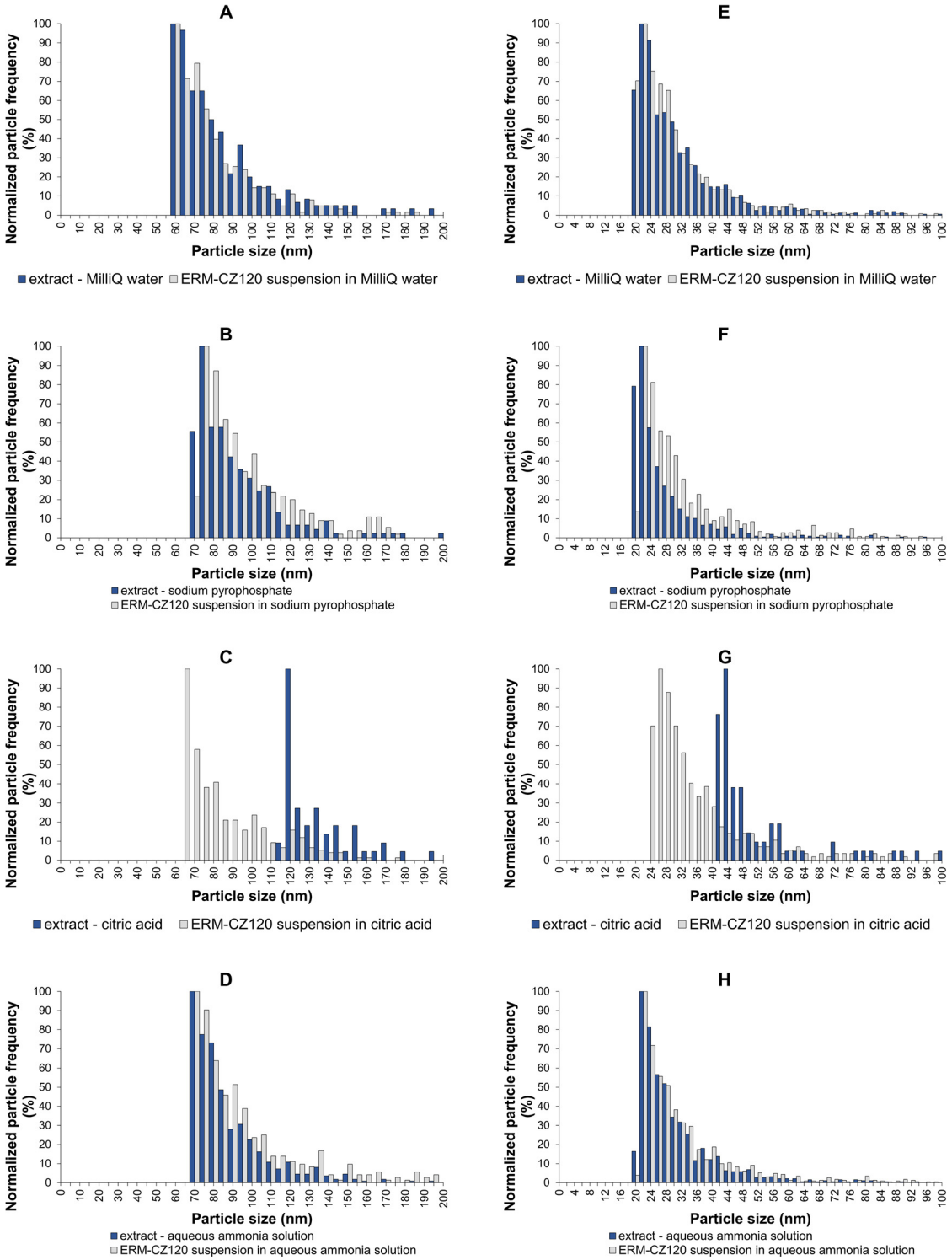

Fig. 2 Particle size distribution obtained by spICP-MS for Zn- and Pb-containing NPs in ERM-CZ120 extracted from PM_{10} filters using different extraction solvents. Zn-containing NPs are presented in Figures (A–D), and Pb-containing NPs are presented in Figures (E–H). The particle size distribution of ERM-CZ120 suspended in the relevant extraction solvent is presented for comparison (grey histograms).

culated for each PM_{10} sample collected in the upper Meža Valley (Table S8†). The average values for location 1 (samples 1–3) and location 2 (samples 4–7) were calculated and compared to the annual limit value of Pb in airborne PM. The average total Pb concentration at location 1 (the year 2018) was 139 ng m^{-3}, while at location 2 (the year 2021) it was 504 ng m^{-3}. Samples 4 and 5, with Pb concentrations of 634 ng m^{-3} and 660 ng m^{-3}, respectively, were the only samples to exceed

Table 2 Total Zn and Pb mass concentrations, particle number and mass concentration, mean particle size, and mass fraction of Zn- and Pb-containing NPs in PM_{10} samples collected in the upper Meža Valley. Total Zn and Pb mass concentrations were determined by ICP-MS with a repeatability better than 3%, while the other parameters were determined by spICP-MS and represent the average values with the standard deviation of two replicates

Sample	Total mass conc. (mg kg^{-1})	Particle number conc. (particles per kg)	Particle mass conc. (mg kg^{-1})	Mean particle size (nm)	Mass fraction of NPs (%)
	Zn				
1a	857 ± 26	$(2.30 \pm 0.81) \times 10^{12}$	29.8 ± 18.0	105 ± 6	3.47
1b	964 ± 29	$(2.31 \pm 0.12) \times 10^{12}$	36.6 ± 14.4	106 ± 2	3.79
2a	1122 ± 34	$(2.93 \pm 0.28) \times 10^{12}$	9.76 ± 2.19	89 ± 2	0.870
2b	921 ± 28	$(2.72 \pm 0.72) \times 10^{12}$	16.2 ± 1.2	96 ± 1	1.76
3a	998 ± 30	$(2.13 \pm 0.81) \times 10^{12}$	8.20 ± 3.06	88 ± 7	0.822
3b	1028 ± 31	$(1.87 \pm 0.00) \times 10^{12}$	6.15 ± 0.58	90 ± 3	0.598
4	1476 ± 44	$(7.47 \pm 1.38) \times 10^{12}$	30.1 ± 1.6	90 ± 5	2.04
5	1676 ± 50	$(6.31 \pm 2.30) \times 10^{12}$	26.1 ± 1.2	92 ± 8	1.55
6	1335 ± 40	$(5.05 \pm 0.75) \times 10^{12}$	33.1 ± 3.6	100 ± 4	2.48
7	1848 ± 55	$(6.67 \pm 0.75) \times 10^{12}$	39.0 ± 4.6	96 ± 3	2.11
	Pb				
1a	5560 ± 167	$(1.54 \pm 0.25) \times 10^{14}$	30.6 ± 3.4	27 ± 0	0.550
1b	5883 ± 176	$(1.72 \pm 0.18) \times 10^{14}$	26.3 ± 6.2	26 ± 0	0.447
2a	4372 ± 131	$(1.61 \pm 0.06) \times 10^{14}$	32.0 ± 12.4	27 ± 1	0.732
2b	4251 ± 128	$(1.46 \pm 0.06) \times 10^{14}$	30.8 ± 1.6	27 ± 0	0.724
3a	3942 ± 118	$(1.88 \pm 0.15) \times 10^{14}$	40.1 ± 34.2	25 ± 2	1.02
3b	3798 ± 114	$(1.76 \pm 0.24) \times 10^{14}$	65.4 ± 37.4	28 ± 2	1.72
4	14 733 ± 442	$(3.36 \pm 0.45) \times 10^{14}$	131 ± 10	30 ± 1	0.888
5	18 846 ± 565	$(3.23 \pm 0.03) \times 10^{14}$	123 ± 49	30 ± 1	0.650
6	26 413 ± 792	$(2.04 \pm 0.09) \times 10^{14}$	81.3 ± 1.7	30 ± 0	0.308
7	22 925 ± 688	$(1.96 \pm 0.05) \times 10^{14}$	65.2 ± 22.4	30 ± 1	0.285

the annual limit value for Pb, which aligns with the presence of Saharan dust and elevated PM_{10} levels. Similarly, the average total Zn concentration was higher in 2021 (41.8 ng m^{-3} at location 2) than in 2018 (28.3 ng m^{-3} at location 1).

3.3. Determination of metal-containing NPs extracted from PM_{10} samples of the upper Meža Valley

The presence of metal-containing NPs in the extracts of PM_{10} samples from the upper Meža Valley was assessed by using the optimized extraction procedure (see Section 3.1) followed by spICP-MS analysis. The analysis confirmed the presence of Zn- and Pb-containing NPs in all of the analyzed extracts, indicating their occurrence in PM_{10} samples. The corresponding particle number and mass concentration, mean particle size, and mass fraction of the extracted Zn- and Pb-containing NPs are presented in Table 2. The highest number concentrations of Zn- and Pb-containing NPs were observed in PM_{10} samples 4, 5, 6, and 7, all from location 2. The particle number concentrations of Zn-containing NPs ranged between 1.87×10^{12} particles per kg (location 1) and 7.47×10^{12} particles per kg (location 2), and between 1.46×10^{14} particles per kg (location 1) and 3.36×10^{14} particles per kg (location 2) for Pb-containing NPs. There was a significant difference (*t*-test, $p < 0.05$) between the particle number concentration of Zn-containing NPs in PM_{10} samples collected in June and August 2021 (4, 5, 6, 7) and October 2018 (1, 2, 3). The mass concentrations of Zn-containing NPs ranged between 6.15 mg kg^{-1} (location 1) and 39.0 mg kg^{-1} (location 2), and between 26.3 mg kg^{-1} (location 1) and 131 mg kg^{-1} (location 2) for Pb-containing NPs. A significant difference (*t*-test, $p < 0.05$) was observed in the particle mass concentration of Pb-containing NPs between PM_{10} samples collected from location 1 and those from location 2. In contrast, the mass concentrations of Zn-containing NPs did not differ significantly between the two locations. The calculation of the Pearson correlation coefficient (PCC) to evaluate potential relationships among various particle parameters (including particle mass and number concentration, as well as total element concentration) in each PM_{10} sample revealed a very strong correlation between the number and mass concentrations of Pb-containing NPs (PCC = 0.95). Additionally, total Zn concentration exhibited a very strong correlation with the number concentration of Zn-containing NPs (PCC = 0.91), while total Pb concentration showed a strong correlation with the mass concentration of Pb-containing NPs (PCC = 0.64).

The mean particle size of Zn-containing NPs ranged from 88 nm to 106 nm, and from 25 nm to 30 nm for Pb-containing NPs. The mass fraction of (nano)particulate Zn extracted from PM_{10} samples ranged from 0.598 to 3.79%. The highest mass fraction of Zn NPs was found in sample 1, consistent with the presence of larger Zn-containing NPs in this sample (Fig. 3A). In contrast, the size distribution of Pb-containing NPs (Fig. 3B) and the percentage of Pb present in NP form (0.285–1.72%) across different samples showed smaller variability. Interestingly, the mass fraction of Pb-containing NPs in the collected PM_{10} samples was significantly lower than in the ERM-CZ120 extracts (7.12 ± 0.88%, see Table 1). This suggests that Pb in the PM_{10} samples from the upper Meža Valley was likely bound to coarser airborne particles,[19] which were less efficiently extracted into the solution, leading to a smaller

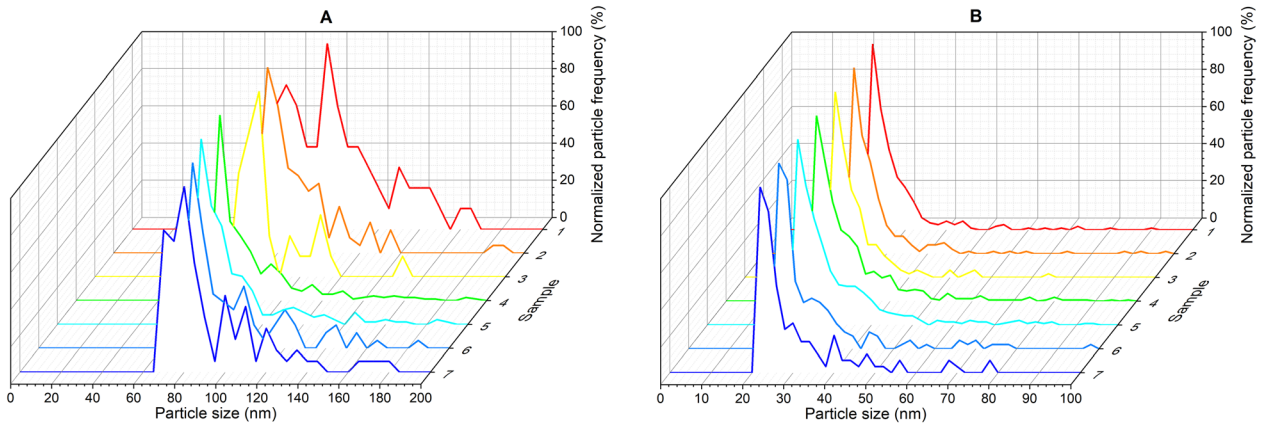

Fig. 3 Particle size distribution of (A) Zn-, and (B) Pb-containing NPs in PM_{10} samples collected in the upper Meža Valley. The samples were extracted from PM_{10} filters using an optimized extraction procedure and analyzed by spICP-MS.

mass fraction of Pb-containing NPs. There was no significant difference (*t*-test, $p > 0.05$) between the mass fraction of Zn- and Pb-containing NPs in PM_{10} samples collected in June and August 2021 (4, 5, 6, 7) and October 2018 (1, 2, 3).

To further assess the anthropogenic contribution to the Zn- and Pb-containing NPs in the studied PM_{10} samples, both particle mass concentrations as well as total element concentrations were normalized to the total aluminum (Al) concentration determined in each sample. The samples were compared based on the location (or year of sampling), and whether the Saharan dust was present at the time of sampling. The ratios of total concentrations (Zn/Al and Pb/Al) and particle mass concentrations (Zn NPs/Al and Pb NPs/Al) differed across samples collected on different days (Table S9†). At location 1, sample 3 had the highest Zn/Al, Pb/Al, and Pb NPs/Al ratios, while its Zn NPs/Al ratio was comparable with those of samples 1 and 2. Sample 3 also showed the highest Pb NPs/Al ratio among all 7 samples. This suggests the anthropogenic contribution of Pb-containing NPs in sample 3 is more likely. At location 2, sample 6 had the highest values for all four ratios, again indicating an anthropogenic origin of these particles. No significant difference was observed between samples collected in 2018 and 2021, likely due to the high variability in daily measurements. When comparing samples 4 and 5 (collected during the presence of Saharan dust) with other samples, they showed lower Zn/Al, Pb/Al, Zn NPs/Al ratios, with similar or lower Pb NPs/Al ratios. However, the only significant difference (*t*-test, $p < 0.05$) was observed for the Zn NPs/Al ratio.

3.4. SEM-EDS analysis of metal-containing NPs extracted from PM_{10} samples of the upper Meža Valley

To complement the spICP-MS results, extracts of PM_{10} filters from the upper Meža Valley were analyzed using SEM-EDS to determine the shape, size, and elemental composition of (nano)particles that contained Zn and Pb. The analysis revealed that Zn- and Pb-containing particles of different sizes, shapes, and elemental compositions were present in all the investigated samples, with most being multi-elemental, containing elements such as Pb, Zn, S, O, Fe, Sn, Cr, and Ca (Fig. 4). Based on the EDS spectra, Pb-containing particles were almost solely composed of Pb sulphate (Fig. 4A–C), while Zn was found in oxides with minor amounts of Ca and Al impurities (Fig. 4H) or Fe-Al oxides with minor amounts of Zn, Cr, and Mg impurities (Fig. 4G and I). Some particles also contained minor atomic percentages of both Pb and Zn (Fig. 4D–F), while the high Si content in the EDS spectra of samples shown in Fig. 4A, E and F was a result of the silicon plate used as a base for sample droplet deposition and the silicon filter fibers. Previous studies on metal-bearing phases in the attic and household dust[19] and snow[31] from the upper Meža Valley area suggest that the chemical composition of metal-containing particles could reflect their sources. According to these studies, the presence of Pb sulphate particles in our samples may suggest primary Pb-smelting, while Fe-oxides with traces of Zn, Cu, and Pb may be associated with mining and mechanical processing of mine waste.[32] However, as SEM-EDS can only provide rough qualitative data on particle composition, accurate identification of their sources remains challenging.

SEM images in Fig. 4 further show that both Zn- and Pb-containing particles exhibited spherical and rectangular shapes. Pb-containing particles were predominantly arranged individually, while Zn-containing and mixed Pb–Zn particles were also aggregated. Although larger particles and the aggregates/agglomerates (in the μm range) were present, the study focused only on particles in the nanometer scale to allow direct comparison with the spICP-MS results. SEM-EDS identified particle sizes ranging from 93 nm to 900 nm (Fig. 4), which were larger than the particles detected by spICP-MS analysis. Comparing SEM results with spICP-MS data is not straightforward due to biases in particle size determination from spICP-MS, which relies on assumptions about particle composition, density, and shape that are often unknown in environmental samples. The mean particle sizes determined by spICP-MS in the PM_{10} filter extracts from the upper Meža Valley were therefore only indicative, based on the assumption

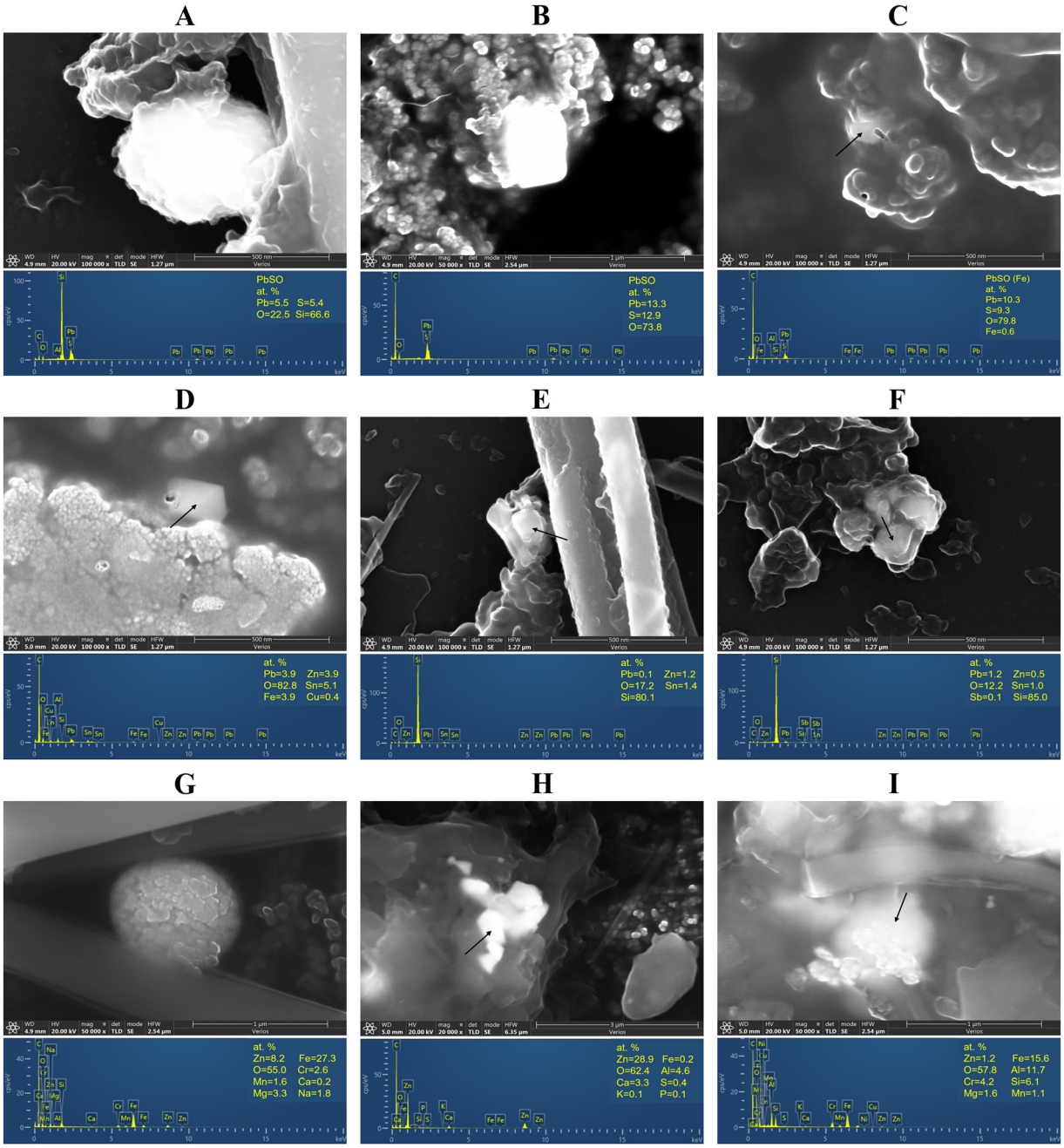

Fig. 4 SEM images, EDS spectra, and elemental composition of particles in filtered extracts of PM_{10} samples from the upper Meža Valley. Pb-containing particles are presented in Figures (A–C), a mix of both in Figures (D–F), and Zn-containing particles are presented in Figures (G–I).

of spherical particles consisting solely of Zn or Pb, while EDS spectra revealed that particles were primarily sulphates and oxides with minor Zn and/or Pb content. As the molar fraction of the element in NP decreases (from NPs containing the pure element to NPs containing relevant sulphates/oxides), the particle diameter calculated by spICP-MS increases. For example, assuming a Pb sulphate ($PbSO_4$) composition with a mass fraction of Pb 0.684 and density of 6.29 g cm^{-3}, the mean particle diameter would increase to 37 ± 1 nm, resulting in a particle size distribution containing particles as large as 100 nm (Fig. S8†). However, even the recalculated sizes of $PbSO_4$ particles determined by spICP-MS were, in general, still smaller than those observed by SEM (Fig. 4A–C). Discrepancies in particle size measurements between spICP-MS and SEM-EDS can be further attributed to the complexity of the sample matrix combined with the physical limitations of the SEM-EDS method. The PM_{10} filter samples contained a variety of particles of different compositions and sizes, with only a small fraction comprising Zn and Pb, making their identification by SEM-EDS difficult. The requirement for dry samples in SEM

led to a potential increase in particle size due to recrystallization, and the use of sodium pyrophosphate created a thin film that further hindered particle detection (Fig. S9†). Additionally, the resolution of the EDS (~1 μm) posed challenges for analyzing small particles in such real environmental samples. All these limitations highlight the importance of combining both spICP-MS and SEM-EDS techniques for a comprehensive analysis of airborne metal-containing NPs at low environmental concentrations.

4. Conclusions

This work aimed to refine an analytical procedure for the extraction and spICP-MS detection of metal-containing NPs in airborne PM_{10} particles from areas with mining, smelting, and similar industries. The two-hour ultrasound-assisted extraction of PM_{10} filters in 10 mM sodium pyrophosphate gave the highest extraction efficiency of all the extraction solvents tested without changing the original properties of NPs. Although extraction in 1% citric acid resulted in comparable or even higher extraction efficiencies for the total concentrations of Zn and Pb, spICP-MS results showed that 1% citric acid caused the partial dissolution of NPs. The proposed analytical procedure was demonstrated to be fit for purpose for real PM samples, as shown by its application to Zn- and Pb-containing NPs in PM_{10} samples from the upper Meža Valley, Slovenia, a former mining and smelting area. To the best of our knowledge, this study is the first to report the presence, concentration, and size of metal-containing NPs in PM_{10} from this region. The total Zn concentration ranged from 857 to 1848 mg kg^{-1}, while the total Pb content varied between 3798 and 26 413 mg kg^{-1}. In the PM_{10} extracts, only a small fraction of Zn (0.598–3.79%) and Pb (0.285–1.72%) was found in the form of NPs. SEM-EDS analysis further confirmed the presence of particles of different sizes, shapes, and chemical compositions, primarily as sulphates and oxides that at least partially contain Zn and/or Pb, or have these elements attached to their surface. While direct size comparisons between SEM-EDS and spICP MS are not possible, the spICP-MS method proved sensitive enough to detect metal-containing NPs at concentrations as low as those found in PM_{10} samples. While no established or recommended annual limit values exist for metal-containing NPs in airborne PM, the presence of Zn- and Pb-containing particles in PM_{10} filters from the upper Meža Valley, despite being only a small fraction of the total Zn and Pb, suggests that the local population is exposed to these airborne NPs with a potential risk for their health.

This work has highlighted the importance of NPs analysis and the need for methods that can efficiently extract metal-containing NPs from environmental samples. While the existing literature reports an extraction efficiency of around 2%, this work improved it to around 9% for Zn- and 14% for Pb-containing NPs. However, further method improvement is necessary, alongside the development of matrix-matched standard reference materials.

Author contributions

Conceptualization, T.Ž., J.V., T.Z.; methodology, T.Ž., J.V., T.Z.; validation, J.V., T.Z.; formal analysis, T.Ž., B.A.; investigation, T.Ž., J.V., T.Z.; resources, T.Z.; data curation, T.Ž., J.V., T.Z.; writing – original draft preparation, T.Ž.; writing – review and editing, J.V., T.Z., B.A.; visualization, T.Ž., J.V., B.A.; supervision, J.V., T.Z.; project administration, T.Z.; funding acquisition, T.Z. All authors have read and agreed to the published version of the manuscript.

Data availability

The data supporting this article have been included as part of the ESI.†

Conflicts of interest

There are no conflicts of interest to declare.

Acknowledgements

This research was funded by the Slovenian Research and Innovation Agency – ARIS: Program (P1-0143), Young research program (PR-10487), research project DISCOVER (J1-60008), and CRP Project – Identification of Pb sources in the upper Meža Valley based on Pb isotope composition (V1-1939).

The authors would also like to thank I. Kranjc, J. Turšič, and J. Burger from the Slovenian Environment Agency (ARSO) for providing the PM_{10} samples from the upper Meža Valley.

References

1 K. Bodor, M. M. Micheu, Á. Keresztesi, M. V. Birsan, I. A. Nita, Z. Bodor, *et al.*, Effects of PM_{10} and Weather on Respiratory and Cardiovascular Diseases in the Ciuc Basin (Romanian Carpathians), *Atmosphere*, 2021, **12**(2), 289, DOI: 10.3390/atmos12020289.

2 C. Liu, R. Chen, F. Sera, A. M. Vicedo-Cabrera, Y. Guo, S. Tong, *et al.*, Ambient Particulate Air Pollution and Daily Mortality in 652 Cities, *N. Engl. J. Med.*, 2019, **381**(8), 705–715, DOI: 10.1056/NEJMoa1817364.

3 Y. Yang, M. Vance, F. Tou, A. Tiwari, M. Liu and M. F. Hochella, Nanoparticles in road dust from impervious urban surfaces: distribution, identification, and environmental implications, *Environ. Sci.: Nano*, 2016, **3**(3), 534–544, DOI: 10.1039/c6en00056h.

4 J. Csavina, J. Field, M. P. Taylor, S. Gao, A. Landázuri, E. A. Betterton, *et al.*, A review on the importance of metals and metalloids in atmospheric dust and aerosol from mining operations, *Sci. Total Environ.*, 2012, **433**, 58–73, DOI: 10.1016/j.scitotenv.2012.06.013.

5 A. D. Woolf, R. Goldman and D. C. Bellinger, Update on the Clinical Management of Childhood Lead Poisoning, *Pediatr. Clin. North Am.*, 2007, **54**(2), 271–294, DOI: 10.1016/j.pcl.2007.01.008.

6 K. Folens, T. Van Acker, E. Bolea-Fernandez, G. Cornelis, F. Vanhaecke, G. D. Du Laing, *et al.*, Identification of platinum nanoparticles in road dust leachate by single particle inductively coupled plasma-mass spectrometry, *Sci. Total Environ.*, 2018, **615**, 849–856, DOI: 10.1016/j.scitotenv.2017.09.285.

7 A. P. Gondikas, F. V. D. Kammer, R. B. Reed, S. Wagner, J. F. Ranville and T. Hofmann, Release of TiO_2 Nanoparticles from Sunscreens into Surface Waters: A One-Year Survey at the Old Danube Recreational Lake, *Environ. Sci. Technol.*, 2014, **48**(10), 5415–5422, DOI: 10.1021/es405596y.

8 A. K. Venkatesan, B. T. Rodríguez, A. R. Marcotte, X. Bi, J. Schoepf, J. F. Ranville, *et al.*, Using single-particle ICP-MS for monitoring metal-containing particles in tap water, *Environ. Sci.: Water Res. Technol.*, 2018, **4**(12), 1923–1932, DOI: 10.1039/c8ew00478a.

9 F. Laborda, E. Bolea and J. Jiménez-Lamana, Single Particle Inductively Coupled Plasma Mass Spectrometry: A Powerful Tool for Nanoanalysis, *Anal. Chem.*, 2014, **86**(5), 2270–2278, DOI: 10.1021/ac402980q.

10 D. Mozhayeva and C. Engelhard, A critical review of single particle inductively coupled plasma mass spectrometry – A step towards an ideal method for nanomaterial characterization, *J. Anal. At. Spectrom.*, 2020, **35**(9), 1740–1783, DOI: 10.1039/c9ja00206e.

11 T. Cen, L. Torrent, A. Testino and C. Ludwig, Rotating disk diluter hyphenated with single particle ICP-MS as an online dilution and sampling platform for metallic nanoparticles characterization in ambient aerosol, *J. Aerosol Sci.*, 2024, **175**, 106283, DOI: 10.1016/j.jaerosci.2023.106283.

12 G. D. Bland, M. Battifarano, Q. Liu, X. Yang, D. Lu, G. Jiang, *et al.*, Single-Particle Metal Fingerprint Analysis and Machine Learning Pipeline for Source Apportionment of Metal-Containing Fine Particles in Air, *Environ. Sci. Technol. Lett.*, 2023, **10**(11), 1023–1029, DOI: 10.1021/acs.estlett.2c00835.

13 D. Torregrosa, G. Grindlay, M. De La Guardia, L. Gras and J. Mora, Determination of metallic nanoparticles in air filters by means single particle inductively coupled plasma mass spectrometry, *Talanta*, 2023, **252**, 123818, DOI: 10.1016/j.talanta.2022.123818.

14 M. L. Avramescu, K. Casey, C. Levesque, J. Chen, C. Wiseman and S. Beauchemin, Identification and quantification of trace metal(loid)s in water-extractable road dust nanoparticles using SP-ICP-MS, *Sci. Total Environ.*, 2024, **924**, 171720, DOI: 10.1016/j.scitotenv.2024.171720.

15 S. Baur, T. Reemtsma, H. J. Stärk and S. Wagner, Surfactant assisted extraction of incidental nanoparticles from road runoff sediment and their characterization by single particle-ICP-MS, *Chemosphere*, 2020, **246**, 125765, DOI: 10.1016/j.chemosphere.2019.125765.

16 C. Gómez-Pertusa, M. C. García-Poyo, G. Grindlay, R. Pedraza, M. A. Yáñez and L. Gras, Determination of metallic nanoparticles in soils by means spICP-MS after a microwave-assisted extraction treatment, *Talanta*, 2024, **272**, 125742, DOI: 10.1016/j.talanta.2024.125742.

17 M. Gosar and M. Miler, Anthropogenic metal loads and their sources in stream sediments of the Meža River catchment area (NE Slovenia), *Appl. Geochem.*, 2011, **26**(11), 1855–1866, DOI: 10.1016/j.apgeochem.2011.06.009.

18 N. Finzgar, E. Jez, D. Voglar and D. Lestan, Spatial distribution of metal contamination before and after remediation in the Meza Valley, Slovenia, *Geoderma*, 2014, **217–218**, 135–143, DOI: 10.1016/j.geoderma.2013.11.011.

19 M. Miler and M. Gosar, Assessment of contribution of metal pollution sources to attic and household dust in Pb–polluted area, *Indoor Air*, 2019, **29**(3), 487–498, DOI: 10.1111/ina.12548.

20 T. Goltnik, J. Burger, I. Kranjc, J. Turšič and T. Zuliani, Potentially Toxic Elements and Pb Isotopes in Mine-Draining Meža River Catchment (NE Slovenia), *Water*, 2022, **14**(7), 998, DOI: 10.3390/w14070998.

21 M. Ivartnik, H. Pavlič, N. Hudopisk, M. Simetinger, J. Ploder and B. Hočevar, *et al.*, *Poročilo o izvajanju programa ukrepov za izboljšanje kakovosti okolja v Zgornji Mežiški dolini za leto 2022*, NIJZ OE Ravne, Ravne na Koroškem, 2022.

22 M. P. Beeston, J. Teun Van Elteren, V. S. Šelih and R. Fairhurst, Characterization of artificially generated PbS aerosols and their use within a respiratory bioaccessibility test, *Analyst*, 2010, **135**(2), 351–357, DOI: 10.1039/B910429A.

23 M. C. Pietrogrande, D. Bacco, A. Trentini and M. Russo, Effect of filter extraction solvents on the measurement of the oxidative potential of airborne $PM_{2.5}$, *Environ. Sci. Pollut. Res.*, 2021, **28**(23), 29551–29563, DOI: 10.1007/s11356-021-12604-7.

24 H. E. Pace, N. J. Rogers, C. Jarolimek, V. A. Coleman, C. P. Higgins and J. F. Ranville, Determining Transport Efficiency for the Purpose of Counting and Sizing Nanoparticles via Single Particle Inductively Coupled Plasma Mass Spectrometry, *Anal. Chem.*, 2011, **83**(24), 9361–9369, DOI: 10.1021/ac201952t.

25 M. Piaścik, E. Perez Przyk and A. Held, The certification of the mass fractions of arsenic, cadmium, nickel and lead in fine dust (PM10-like matrix): certified reference material ERM-CZ120. LU: Publications Office, European Commission. Joint Research Centre. Institute for Reference Materials and Measurements, 2010, Available from: https://data.europa.eu/doi/10.2787/31636.

26 D. Bec, D. Ciglenečki, P. Dolšak Lavrič, M. Gjerek, T. Koleša and M. Logar, *et al.*, *Kakovost zraka v Sloveniji v letu 2021*, ARSO, Ljubljana, 2022.

27 Q. Wang, G. Zhuang, J. Li, K. Huang, R. Zhang, Y. Jiang, *et al.*, Mixing of dust with pollution on the transport path of Asian dust—Revealed from the aerosol over Yulin, the

north edge of Loess Plateau, *Sci. Total Environ.*, 2011, **409**(3), 573–581, DOI: 10.1016/j.scitotenv.2010.10.032.

28 J. Loskot, D. Jezbera, M. Nalezinková, A. H. Šmejkalová, D. Fernandes and J. Komárek, Impact of Saharan dust on particulate matter characteristics in an urban and a natural locality in Central Europe, *Sci. Rep.*, 2024, **14**(1), 32002, DOI: 10.1038/s41598-024-83603-0.

29 WHO global air quality guidelines. Particulate matter (PM2.5 and PM10), ozone, nitrogen dioxide, sulfur dioxide and carbon monoxide.World Health Organization, 2021.

30 Directive 2008/50/EC of the European Parliament and of the Council of 21 May 2008 on ambient air quality and cleaner air for Europe. European Union, 2008.

31 M. Miler and M. Gosar, Assessment of Metal Pollution Sources by SEM/EDS Analysis of Solid Particles in Snow: A Case Study of Žerjav, Slovenia, *Microsc. Microanal.*, 2013, **19**(6), 1606–1619, DOI: 10.1017/S1431927613013202.

32 M. Miler and M. Gosar, Characteristics and potential environmental influences of mine waste in the area of the closed Mežica Pb–Zn mine (Slovenia), *J. Geochem. Explor.*, 2012, **112**, 152–160, DOI: 10.1016/j.gexplo.2011.08.012.